Research Article

Multi-UCAV Cooperative Target Allocation Based on Energy-Reserved Chemical Reaction Algorithm (CNCRO)

Dai Jun-Feng [1] **and Fu Li-Hui** [2]

^{1}Faculty of Electronic Information Engineering, Huaiyin Institute of Technology, Huaian 223003, Jiangsu, China
^{2}Faculty of Automation, Huaiyin Institute of Technology, Huaian 223003, Jiangsu, China

Correspondence should be addressed to Fu Li-Hui; flh3650326@163.com

Aimed at the disadvantages of constrained processing technology in the cooperative target allocation of multiple unmanned combat aircraft (UCAV), the energy-reserved chemical reaction algorithm (CNCRO) is proposed to solve the constrained optimization problems. On the one hand, convert multiple constraint conditions of the multi-UCAV target allocation into optimization targets to transform the constrained processing problem into a multiobjective optimization problem including allocation goals and constrained optimization goals. On the other hand, the energy-reserved chemical reaction algorithm (CNCRO) is proposed, which introduces the environmental energy-reserved variables buffer into the ineffective collision, combination or splitting reactions between single molecule and multimolecules of CNCRO, which is used to boost energy for the low kinetic energy molecules, so as to reduce its kinetic energy in case of invalid collision of molecules and control it to gradually stabilize and converge. At the same time, the splitting reaction is inspired, to greatly change the structure of molecules, promote its search for more solution space, and improve the splitting reaction ability and its global optimization ability. Finally, the simulation experiment is completed by using MATLAB software. The advantages of CNCRO in accuracy are verified by 8 standard test functions, the influence of the weight coefficients in the cooperative target allocation function of UCAV is studied, which are revenue, loss, and voyage, and the target allocation schemes of traditional constrained processing and unconstrained multi-objective optimization methods based on different attack target number C_i and total target number N are investigated, to obtain the control law, which can be used to guide the given parameters with different emphases.

1. Introduction

The cooperative target allocation problem of multi-UCAV is an NP problem of optimization with multiple models, multiple constraints, and increasing complexity [1]. It is used to allocate the attack targets for UCAV, so as to maximize the combat efficiency and minimize the combat cost of the entire UCAV, thus facilitating the rational allocation of force resources to obtain the maximum attack effect. Its main feature is that the constraints are numerous and complex [2]; therefore, the constraint processing technology is the key problem in the process of UCAV cooperative target allocation, not only the constraints of the UAV itself but also the constraints of the cooperative problem should be considered. Currently, the commonly used processing algorithms include genetic algorithm (GA) [3], simulated annealing (SA) [4], ant colony algorithm (ACA) [5]. Among them, literature [6] proposed a genetic algorithm with dynamic crossover rate and mutation rate, which maintained the diversity of the population and avoided premature convergence. Document [7] proposes a hierarchical multiagent optimization algorithm, which combines multiagent optimization algorithm and genetic algorithm (GA) to improve resource utilization. Literature [8] designed a selection algorithm with the centralized iterative interference strategy based on the optimal dynamic response and proposed an allocation algorithm of distributed limited feedback interference resources. Literature [9] enhances the

performance of the genetic algorithm by introducing greedy algorithms. The adaptive ant colony algorithm proposed in literature [10] improves the reliability of the algorithm. Literature [11] uses artificial immune systems to solve the problem. Literature [12] focuses on the interference energy ratio of the interference suppression method and changes the proposed model into a convex optimization problem. Document [13] proposes a decision-making algorithm for resource allocation based on hierarchical reinforcement learning of bootstrap experts to solve the problem of interference decisions. In addition, considering long-term benefits and current benefits, the authors of [14] propose a distributed deep compression algorithm and a distributed quick compression algorithm and adopt a distributed framework to complete task optimization. In view of the rapid response characteristics of multiple UAVs in a dynamic environment, the authors of [15] extend the consensus-based bundling algorithm to quickly allocate new tasks without completely redistributing existing tasks. Based on the task and the UAV group, the authors of [16] establish the state information model of the UAV and UAV group and solve the problem by improving the particle swarm algorithm and distributed auction algorithm. However, in the process of solving problems with these algorithms, solutions that do not meet the constraint conditions are inevitably generated, and premature convergence is easy occurring. At this time, it is generally necessary to use the heuristic information in the constraints to check the solutions, or adopt the methods such as penalty functions and constraint tournaments [17, 18]. Nevertheless, repeated attempts to check the solution in real time will affect the solving speed, and it is difficult to select the penalty factor of the penalty function method, which has problem relevance and is difficult for users to grasp. Other algorithms such as the constraint tournament are always designed for specific problems, which are not universal, and their effects are not good and will increase the time consumption. Therefore, for the application of multi-UCAV cooperative target allocation, this paper regards the constraints in target assignment as multiple targets and transforms the constrained optimization problem composed of n decision variables, single objective function, l inequality constraints, and $m - l$ equality constraints into a nonconstrained multiobjective optimization problem with n decision variables and two objective functions, and the energy-reserved chemical reaction algorithm (CNCRO) is used to optimize and to realize the rational allocation of UCAV cooperative goals under complex constraints.

In this paper, we propose the energy-reserved chemical reaction algorithm (CNCRO) and applied it to the process of UCAV cooperative target allocation. The main novelty of the proposed approach is as follows: (1) the constrained optimization problem is transformed into a multiobjective optimization problem for processing, to avoid the repeated trial of the conventional constrained optimization method. (2) The energy-reserved chemical reaction algorithm (CNCRO) is proposed. The environmental energy-reserved variable buffer is introduced into the ineffective collision, combination or splitting reaction between single and multiple molecules of CNCRO to supplement energy for low kinetic energy molecules and inspire the splitting reaction, to greatly change the molecular structure and promote its search for more solution space, improve the global optimization of CNCRO; (3) the influence of the weight coefficients (ω_1, ω_2, ω_3) of the overall income, the overall loss, and the total flight range in the objective function of UCAV on the allocation scheme is studied through the simulation experiments, and the influence laws of the maximum number of attack targets (C_i) and the total number of targets (N) on the allocation scheme are obtained, which can lay a foundation for the subsequent implementation of target allocation based on different emphases.

The remainder of this paper is organized as follows. In Section 2, we introduce the target allocation model of multi-UCAV, including the problem description and constraint conditions. The processing process of the chemical reaction algorithm for solving the cooperative target assignment of multi-UCAV is introduced in Section 3, including the collision reaction, the splitting reaction, and the combination reaction. In Section 4, the performance of the proposed method is illustrated and compared with some other task allocation algorithms. Section 5 concludes the paper.

2. The Target Allocation Model of Multi-UCAV

2.1. Problem Description. Assuming that the sets of multi-UCAV are $U_i (U_i \in U, \quad i = 1, 2, \ldots N)$, the multiple targets scattered in different locations are $(T_k \in T, \quad k = 1, 2, \ldots M)$, and then, the target assignment problem of multi-UCAV is described as assigning existing targets to all attackers of the system in the shortest time. Taking the minimum loss to obtain the maximum benefit and the minimum flight range as the indexes to evaluate the effectiveness of the attack aircraft, the objective function is given as follows:

$$
\begin{aligned}
\max(f(x)) &= \omega_1 \cdot E - \omega_2 \cdot G - \omega_3 \cdot D \\
&= \omega_1 \sum_{i=1}^{N} \sum_{k=1}^{M} x_{ik} \cdot P_{ik} \cdot E_k - \omega_2 \sum_{i=1}^{N} \sum_{k=1}^{M} x_{ik} \cdot Q_{ik} \cdot V_i - \omega_3 \sum_{i=1}^{N} \sum_{k=1}^{M} x_{ik} \cdot D_{ik},
\end{aligned}
\tag{1}
$$

where x_{ik} is the decision variable which defined as

$$x_{ik} = \begin{cases} 1; t \arg et \, k \text{ is assigned to attacker } i, \\ 0; \, t \arg et \, k \text{ is not assigned to attacker } i. \end{cases} \quad (2)$$

P_{ik} is the killing probability of the attacker U_i to the target T_k; E_k is the value of objectives T_k; E is the total benefit obtained by UCAV after attacking all targets; G is the overall loss of the entire attack fleet; D is the total flight range of UCAV; Q_{ik} is the probability of death when the attacker U_i attacks the target T_k; V_i is the value of the *ith* attack aircraft; D_{ik} is the flight range while the *ith* aircraft U_i attack the target T_k; $\omega_1, \omega_2,$ and ω_3 are the weight coefficient of income, loss, and flight range, respectively.

2.2. The Constraint Conditions.
The constraint conditions for multi-UCAV are as follows:

(1) $\sum_{i=1}^{N} x_{ik} = 1$, which represents that each target is assigned to only one attacker

(2) $1 \le \sum_{k=1}^{M} x_{ik} \le C_i$, which means that each attacker must be assigned one target and attack C_i target at most

(3) $\sum_{i=1}^{N} \sum_{k=1}^{M} x_{ik} = T$, which means that all targets are assigned to the group of attack aircraft, T is the collection of multiple targets

2.3. The Handling Method of Constraint Conditions.
The above problem is a single objective function composed of n decision variables, which is a constrained optimization problem with multiple constraints. The focus of this paper is to transform it into an unconstrained multiobjective optimization problem and use a chemical reaction algorithm to optimize it.

First, according to the constraint conditions of the co-operative target assignment task of UCAV described above, inequality constraint conditions $g_j(x)$ and equality constraint conditions $h_j(x)$ are constructed, so that

$$Y_j(x) = \begin{cases} \max\{0, g_j(x)\}; 1 \le j \le l(l = 2), \\ |h_j(x)|; l + 1 \le j \le m(m = 4), \end{cases} \quad (3)$$

where $g_j(x)$ and $h_j(x)$ are specifically defined as

$$g_1(x) = 1 - \sum_{k=1}^{M} x_{ik},$$

$$g_2(x) = \sum_{k=1}^{M} x_{ik} - C_i,$$

$$h_3(x) = \sum_{i=1}^{N} x_{ik} - 1, \quad (4)$$

$$h_4(x) = \sum_{i=1}^{N} \sum_{k=1}^{M} x_{ik} - T.$$

Then,

$$Y(x) = \sum_{j=1}^{4} Y_j(x). \quad (5)$$

Thus, the constraint conditions of multi-UCAV target assignment are transformed into a single objective function. So, two-objective vectors $F(x)$ are formed by $Y(x)$ and $f(x)$ as follows:

$$F(x) = (f(x), Y(x)). \quad (6)$$

So far, a constrained optimization problem consisting of n decision variables, single objective function, l inequality constraints, and $m - l$ equality constraints has been transformed into an unconstrained multiobjective optimization problem with n decision variables and two-objective functions; therefore, the objective function is redefined as

$$\max(F(x)) = \max(f(x), Y(x)). \quad (7)$$

In this paper, the constrained optimization problem is transformed into a multiobjective optimization problem for processing. The main purpose is to avoid the repeated trial for the real-time check of the solution in the conventional constrained optimization method, as well as the problems such as the difficulty in selecting penalty factors and the increasing of time consumption. However, this method is fundamentally different from the conventional multi-objective optimization problem [18]. For the conventional multiobjective optimization problem, its purpose is to find an optimal solution set with uniform distribution and good diversity, and in this paper, $F(x)$ degenerates into a single objective optimization problem $Y(x) = 0$, and its optimal solution is still one point, which is simpler and more reliable to deal with.

3. The Chemical Reaction Algorithm for Solving Multi-UCAV Cooperative Target Assignment

Chemical reaction optimization (CRO) is a heuristic optimization algorithm with strong global optimization ability [19], which originates from the basic process of molecular reaction in the chemical field. Based on the continuous changes in molecular structure and energy in chemical reactions and the characteristics of energy conservation law, Lam and other scholars were inspired and proposed the algorithm in 2009. Subsequently, Lam used the Markov chain to prove the convergence of the algorithm under the total energy and molecular reaction [19]. In 2011, Lam et al. proposed a real-coded chemical reaction optimization algorithm (RCCRO) [20] to solve the optimization problem of solution space in the multidimensional real number domain, which make up for the problem that the conventional algorithm can only solve the optimization of solution space in the discrete domain. So far, the CRO algorithm has received the attention of scholars and has been widely used in the fields of the spectrum allocation of radio systems and network computing [21], and its global optimization ability has also been fully confirmed.

After the constraint optimization problem of UCAV is transformed into a multiobjective problem, how to balance the feasible solution and the infeasible solution becomes particularly important. If the optimization population after entering the feasible domain does not have enough diversity, then the search will focus on a part of the feasible domain, so that the whole population is easily trapped in local optimization. By simulating the interaction between molecules in chemical reactions, CRO achieves a low-energy steady state which has the ability of distributed, parallel, large-scale, and fast global search, so it is suitable for solving multiobjective optimization problems [21]. Based on the traditional chemical reaction algorithm, the energy-reserved chemical reaction algorithm (CNCRO) is proposed in this paper. In the reaction process, the energy-driven method (the molecular with large kinetic energy reacts violently and the molecular with small kinetic energy tends to be stable) is used to increase the diversity of molecular structure through four simple chemical reaction operations, mainly including ineffective collision, combination or splitting reactions of single and multiple molecules. In addition, in the ineffective collision and splitting reaction between a single molecule and the container wall, the environmental energy-reserved variables (buffer) are used to supplement energy for low kinetic energy molecules, so that when an ineffective collision occurs, buffer is utilized to store energy, and the current kinetic energy of the colliding molecule is reduced and gradually tends to be stable; at the same time, the splitting reaction is inspired by using buffer to greatly change the structure of the single molecule to increase the possibility of drastic changes in the molecular structure, improve its splitting reaction ability, make it search more solution spaces, and improve the global optimization ability of the algorithm. Finally, for the cooperative target assignment task of multi-UCAV, CNCRO is used to effectively deal with the multiobjective optimization constraint problem based on UCAV.

3.1. The Ineffective Collision Reaction between Single Molecule and the Walls of Container.
During the movement of a single molecule, the process of rebound after collision with the container wall is defined as the invalid collision reaction between the single molecule and the container wall, which is referred to as the invalid collision reaction with the wall. When an ineffective collision with the wall occurs, some properties of the molecule will change, and the molecular structure will also change at the same time. However, the collision is not too violent, so the molecular structure will not change too much.

Assuming that the structure of the molecule is ω before the ineffective collision reaction with the wall occurs, and the new molecular structure is ω' after the ineffective collision, the acquisition method of new structure is as follows:

$$\omega' = N(\omega), \tag{8}$$

where $N(\cdot)$ is the domain operation function of the molecule in the potential energy surface.

At the same time, the molecular structure change in this process needs to meet certain energy conditions, which is defined as follows:

$$PE_\omega + KE_\omega \geq PE_{\omega'}, \tag{9}$$

where PE_ω and KE_ω are the molecular potential energy and kinetic energy corresponding to the original molecular structure, respectively; $PE_{\omega'}$ is the molecular potential energy corresponding to the new molecular structure, which are calculated by using the objective function of the optimization object in the algorithm. If the equation (9) is satisfied, the molecular structure is updated. According to the principle of energy conservation, the molecular kinetic energy of the new molecular structure is defined as follows:

$$KE_{\omega'} = (PE_\omega + KE_\omega - PE_{\omega'}) \times q, \tag{10}$$

where q is the random decimal number between loss rate and 1 (loss rate is the lower limit of kinetic energy loss probability which is variable).

When an invalid collision reaction occurs between a single molecule and the container wall, part of the energy will be lost from the molecular reaction to the container environment, which will affect the generation of the optimal solution. To store the lost energy, the environmental energy-reserved variables of buffer are defined in the CNCRO algorithm, which mainly considers the following reasons, and on the one hand, the energy will be continuously lost in the event of an invalid collision of a single molecule, and its kinetic energy needs to be reduced to make it gradually stable and make the system gradually converge. On the other hand, the energy saved by the variable of buffer is used to start the splitting reaction after the single molecule collides with the container wall, which greatly changes the molecular structure to promote the splitting reaction of the single molecule, to ensure it can search for more solutions in the solution space, and improve the global optimization ability of the algorithm. Specifically, it is defined as follows:

$$\text{buffer} = \text{buffer} + (PE_\omega + KE_\omega - PE_{\omega'}) \times (1 - q). \tag{11}$$

3.2. The Splitting Reaction between Single Molecule and the Walls of Container.
The violent collision between a single molecule and the wall of the container will cause great changes in the structure of molecular, and the process of splitting one molecule into two or more molecules is referred to as a splitting reaction. There are huge differences between the structure of the new molecule and that of the original molecule. The specific algorithm is as follows.

Assuming that the structure of the original molecule is ω, the structure of the new molecule generated by splitting is ω_1 and ω_2, respectively (taking two molecules as an example). If the original molecule has sufficient energy by itself (equation (12)), or has sufficient energy supplemented by the variables of buffer (equation (13)), it can provide sufficient potential energy for the new molecule, and then, the splitting reaction is successful. Otherwise, the algorithm maintains all the

properties of the original molecule, such as the molecular structure and energy parameters.

$$PE_\omega + KE_\omega \geq PE_{\omega_1} + PE_{\omega_2}. \tag{12}$$

Or

$$PE_\omega + KE_\omega + \text{buffer} \geq PE_{\omega_1} + PE_{\omega_2}. \tag{13}$$

If the equation (12) or (13) is satisfied, it is defined as follows:

$$\begin{cases} KE_{\omega_1} = \text{temp} \times k, \\ KE_{\omega_2} = \text{temp} \times (1 - k). \end{cases} \tag{14}$$

where temp = $PE_\omega + KE_\omega - PE_{\omega_1} - PE_{\omega_2}$.

Otherwise, execute equation:

$$\begin{cases} KE_{\omega_1} = (\text{temp} + \text{buffer}) \times m_1 m_2, \\ KE_{\omega_2} = (\text{temp} + \text{buffer} - KE_{\omega_1}) \times m_3 m_4, \end{cases} \tag{15}$$

where k, m_1, m_2, m_3, m_4 are all random pure decimals.

There are two purposes for setting four random numbers of $m_1 \sim m_4$ in equation (15). First, the energy value of buffer is generally large, so it is necessary to avoid transferring too much energy to a new molecule at one time, which is unfavorable to the convergence of the algorithm. Second, it is necessary to avoid exhausting all the energy buffer at one time, to complete the energy-enlightening effect on other molecules. At this time, buffer is defined as follows:

$$\text{buffer} = \text{temp} + \text{buffer} - KE_{\omega_1} - KE_{\omega_2}. \tag{16}$$

3.3. The Invalid Collision Reaction between Molecules.

The process in which two or more molecules rebound back after colliding with each other is referred to as an invalid collision reaction of intermolecular [20]. Its collision intensity is small, the molecular structure changes little, and the energy changes little. This collision reaction is mainly used to complete the local optimization task, similar to the ineffective collision between a single molecule and the container wall, the changes of molecular structure are obtained by using the neighborhood function $N(\cdot)$, and the molecules in the reaction process meet the energy conservation and do not exchange energy with the container environment; that is, the reaction process is independent of buffer.

Suppose that there is an invalid collision reaction between two molecules, the original molecular structure is ω_1 and ω_2, and the new molecular structure is ω_1' and ω_2'. Then, the reaction can proceed only if the energy transfer conditions of equation (17) are satisfied; otherwise, the original molecular structure and energy properties are maintained.

$$PE_{\omega_1} + KE_{\omega_1} + PE_{\omega_2} + KE_{\omega_2} \geq PE_{\omega_1'} + PE_{\omega_2'}. \tag{17}$$

According to the law of energy conservation, the reaction process is as follows:

$$\begin{cases} KE_{\omega_1'} = \text{temp} \times k, \\ KE_{\omega_2'} = \text{temp} \times (1 - k), \end{cases} \tag{18}$$

where temp = $PE_{\omega_1} + KE_{\omega_1} + PE_{\omega_2} + KE_{\omega_2} - PE_{\omega_1'} - PE_{\omega_2'}$, k is the random decimal between 0 and 1.

3.4. The Combination Reaction after Molecules Colliding with Each Other.

The process in which two or more molecules combine into one molecule after a violent collision is referred to as the combination reaction [20]. It is assumed that the molecular structures before the combination reaction are ω_1, ω_2, the new molecular structure generated after the combination ω. This reaction occurs under the condition of a violent collision, which is similar to the splitting reaction, the molecular structure changes dramatically, and the new molecular structure is very different from the original molecular structure. Similarly, the reaction can be completed only if the energy-changing relationship shown in equation (19) is satisfied; otherwise, the original properties of the two molecules remain unchanged.

$$PE_{\omega_1} + PE_{\omega_2} + KE_{\omega_1} + KE_{\omega_2} \geq PE_\omega. \tag{19}$$

Then, the reaction process is as follows:

$$KE_\omega = PE_{\omega_1} + PE_{\omega_2} + KE_{\omega_1} + KE_{\omega_2} - PE_\omega. \tag{20}$$

If PE_ω and $PE_{\omega_1}, PE_{\omega_2}$ have similar values, the difference of KE_ω and $KE_{\omega_1}, KE_{\omega_2}$ is large; therefore, the combined molecules have large kinetic energy, to ensure their ability to jump out of the local optimal neighborhood in the subsequent reaction and expand the optimization range of the algorithm.

3.5. The Processing Process of CNCRO.

In solving the cooperative target assignment of multi-UCAV, the four reaction processes of the CNCRO are implemented in three stages: initialization phase, iteration phase, and result processing phase. The whole algorithm flow is shown in Figure 1.

The initialization phase is used to complete the initialization of parameters and variables required for the algorithm, including the creation of initial molecules and the initialization of molecular structures and energy values. In the iteration phase, relevant reaction conditions need to be detected to determine the reaction type, and the iteration phase continues until the end conditions are met. The result processing phase is mainly used to read the minimum potential energy molecule and output its molecular structure, which is the global optimal solution.

The pseudocode of the specific processing process is shown in Algorithm 1.

4. The Simulation Experiment and the Comparison of Results

4.1. The Performance Test of the CNCRO Algorithm.

The energy-reserved chemical reaction algorithm (CNCRO) is simulated by MATLAB 2010, and its performance is
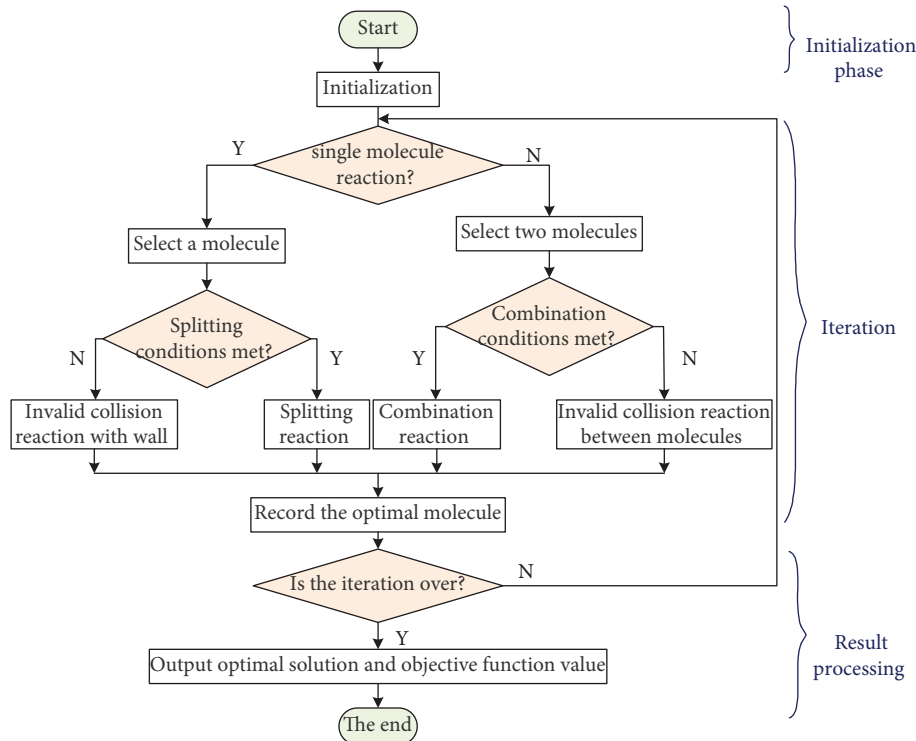
FIGURE 1: The processing flow of energy-reserved chemical reaction algorithm (CNCRO).

compared with the particle swarm optimization (PSO) described in document [22], the parallel genetic algorithm with the elite set (PGA) described in document [23], the simulated annealing genetic algorithm (SAGA) described in document [24], the deep intelligent ant colony optimization algorithm (ACA) described in document [25], and the chemical reaction algorithm (CRO) described in document [26]. The algorithm parameters are shown in Table 1. At the same time, eight standard test functions are used to verify the effectiveness of CNCRO. The test functions are shown in Table 2.

In order to make the experimental results more scientific and effective, eight benchmark functions are given in Table 2, which are divided into three types of functions. The first one is composed of four unimodal functions (f_1, f_2, f_5, f_6) where f_1 and f_5 are simple unimodal function in high-dimensional space, f_2 is a multimodal function, f_6 is unimodal functions with random interference. The second type includes three complex multimode functions (f_3, f_4, f_7), and the last type is the rotation function f_8. The global optimal solution of all test functions is zero.

In the experiment, each problem function is set to 50 dimensions, 6 algorithms are used to optimize 8 standard test functions. Each test function runs independently for 30 times under the same conditions, and the average optimization results and standard deviation are recorded. The experimental results are shown in Table 3.

It can be seen from Table 3 that the CNCRO algorithm can achieve better average value and standard deviation in most functions when solving 50-dimensional problem, especially in the functions of f_1, f_3, f_4, f_5, f_8. For the four unimodal

functions, CNCRO can find the global optimal solution of f_1 and f_5. For f_2 and f_6, the performance of CNCRO is slightly worse than that of PGA but better than other algorithms. For the three multimodal functions, CNCRO can find their optimal solution. Among them, both CNCRO and PGA have the best performance in finding the global optimal solution of f_7. In addition, the optimization effect of CRO for f_3 is better, which is second only to CNCRO, and the effect of PGA in the function of f_4 is slightly worse than that of CNCRO. For the rotation function, CNCRO can find the global optimal solution of f_8, and the performance of PGA in f_8 is slightly worse than that of CNCRO.

In general, CNCRO performs well for most functions except for a few functions. It can be seen that the CNCRO algorithm has strong effectiveness and robustness. By using the environmental energy-reserved variable of $buffer$ to supplement energy for low kinetic energy molecules, the molecular diversity of the CNCRO and the correlation between multiple decision variables are increased, which makes it difficult to fall into local optimization and improve the ability of the new algorithm to solve the complex problems.

4.2. The Simulation Experiment of Multi-UCAV Cooperative Target Allocation Based on CNCRO

4.2.1. The Design of Experimental Parameters. In order to further verify the effectiveness of CNCRO in the cooperative target allocation of multi-UCAV, the following simulation experiments are designed. Assuming that there are 5 attack aircraft (Ua1–Ua5) and 10 targets (Ta1–Ta10), the survival

(1) Define and initialize corresponding parameters, such as the number of molecules (pop size), the lower limit of kinetic energy loss rate (loss rate), the condition threshold (Molecoll), and the initial kinetic energy of molecules (initial KE)

(2) Create molecules based on the number of molecules (popsize)

(3) **For** every molecule **do**
Obtain randomly the molecular structure ω, calculate PE_ω with objective function $f(\omega)$, and initialize KE_ω with initial value of kinetic energy (initial KE)

(4) **end for**

(5) Initialize the environmental energy-reserved variable (buffer = 0)
Create the molecular pointer (M, M_1, M_2)

(6) **while** the end condition of iteration is not satisfied **do**
Generate a random number between 0 and 1 for the temporary variable t

(7) **If** $t >$ Molecoll **then**
Select a molecule of M from the container

(8)   **If** the conditions of classification are met **then**
(M_1, M_2, success) = DecomposeOnWall (M, buffer)

(9)   **If** success == TRUE **then**
Remove the molecule of M from the container while adding the molecules of M_1 and M_2,

(10)   **end if**

(11)   **else**
IneffectiveOnWall (M, buffer)

(12)   **end if**

(13) **else**
Select the molecules of M_1 and M_2 from the container

(14)   **If** the conditions of combination are met **then**
(M, success) = SynthesisInter (M_1, M_2)

(15)   **If** success == TRUE **then**
Remove the molecules of M_1 and M_2 from the container and add the molecule of M at the same time

(16)   **end if**

(17)   **else**
IneffectiveInter (M_1, M_2)

(18)   **end if**

(19) **end if**
Determine whether the potential energy of the new molecule is the lowest and preserve the globally optimal molecule

(20) **end while**

(21) Output the structure and potential energy value of the global optimal molecular, that is the global optimal solution and the objective function value

ALGORITHM 1: The optimization algorithm of CNCRO.

TABLE 1: The parameter settings of each algorithm.

Algorithms	Parameters setting	Reference
PSO	$\omega = 0.7$, $c_1 = c_2 = 1.494$, $V_{\max} = 0.2 \times$ Range	[22]
PGA	Crossover probability = 0.8, mutation probability = 0.6, maximum number of iterations = 1500, initial population size = 120	[23]
SAGA	Initial population size = 100, evolutionary algebra = 200, crossover probability = 0.85, mutation probability = 0.15, annealing bad solution probability = 0.95, attenuation coefficient = 0.85	[24]
ACA	Maximum number of iterations = 1000, maximum number of ants = 25, $\rho = 0.9$, $\alpha = 1$, $\beta = 1$	[25]
CRO	popsize = 25, initial $KE = 0$, loss rate = 0.2, Molecoll = 30	[26]
CNCRO	popsize = 25, initial $KE = 0$, loss rate = 0.2, Molecoll = 20	

probability of the attacker against the target $(1 - Q_{ik})$, the flight range (D_{ik}), the killing probability (P_{ik}), the value of target (E_k), and the value of attack aircraft (V_i) is shown in Tables 4–8, respectively.

4.2.2. The Overall Experimental Results. Matlab 2010 is used for the simulation, and the CNCRO algorithm is compared with conventional target allocation methods (CRO, ACA, SAGA, PGA, PSO). The parameters of the algorithms are shown in Table 1, and the parameters of UCAV cooperative target allocation are shown in Tables 4–8, and the weight coefficients of the income, loss, and flight range in the objective function are set as $\omega_1 = \omega_2 = \omega_3 = 1$, and the maximum number of targets that can be attacked by each UAV is set as $C_i = 4$. Each algorithm has been simulated for 25 times. The curve of the average best solution of the fitness of the objective function is shown in Figure 2. In addition,

TABLE 2: 8 test functions used in the experiment.

Test functions	Search range	Initialization range	f_m	Accept	Name
$f_1(x) = \sum_{i=1}^{n} x_i^2$	[−100, 100]	[50, 100]	0	10^{-6}	Sphere
$f_2(x) = \sum_{i=1}^{n-1} [100(x_{i-1} - x_i^2)^2 + (x_i - 1)^2]$	[−30, 30]	[15, 30]	0	100	Rosenbrock
$f_3(x) = \sum_{i=1}^{n-1} [x_i^2 - 10\cos(2\pi x_i) + 10]$	[−6, 6]	[3, 5]	0	10^{-6}	Rastrigin
$f_4(x) = \frac{1}{4000} \sum_{i=1}^{n-1} [x_i^2 - \prod_{i=1}^{n} \cos(x_i/\sqrt{i}) + 1]$	[−500, 500]	[300, 500]	0	10^{-6}	Griewangk
$f_5(x) = \sum_{i=1}^{n} |x_i| + \prod_{i=1}^{n} |x_i|$	[−10, 10]	[5, 10]	0	10^{-6}	Schwefel 2.2
$f_6(x) = \sum_{i=1}^{n} i x_i^4 + r$ and $[0, 1]_n$	[−1.2, 1.2]	[0.64, 1.28]	0	10^{-6}	Noise
$f_7(x) = -20 \exp(-0.2\sqrt{1/n} \sum_{i=1}^{n} x_i^2) - \exp(1/n) \sum_{i=1}^{n} \cos(2\pi x_i) + 20 + e$	[−32, 32]	[16, 32]	0	10^{-6}	Ackley
$f_8(x) = \sum_{i=1}^{n} |x_i \sin(x_i) + 0.1 x_i|$	[−10, 10]	[5, 10]	0	10^{-6}	Alpine

TABLE 3: The simulation results of CRO, ACA, SAGA, PGA, PSO, and CNCRO.

Problem	Optimal		SAGA	PSO	ACA	CRO	PGA	CNCRO
f_1	0	Mean	$1.50E-01$	$1.32E-01$	$1.15E-01$	$1.30E+00$	$0.65E-01$	$\mathbf{0.40E-01}$
		Std	$1.62E+04$	$1.50E+04$	$1.47E+03$	$0.01E+00$	$0.01E+00$	$\mathbf{0.01E+00}$
f_2	0	Mean	$2.30E+03$	$2.20E+03$	$2.59E+03$	$2.20E+03$	$\mathbf{1.70E+03}$	$0.86E+03$
		Std	$2.20E+02$	$3.00E+02$	$6.50E+01$	$2.00E+01$	$\mathbf{0.00E+00}$	$0.00E+00$
f_3	0	Mean	$6.10E+02$	$6.13E+02$	$6.48E+02$	$4.10E+02$	$10.0E+01$	$\mathbf{3.25E+01}$
		Std	$7.45E+07$	$1.10E+08$	$7.70E+02$	$0.00E+00$	$2.10E-01$	$\mathbf{2.50E-01}$
f_4	0	Mean	$2.40E-02$	$1.51E-02$	$1.87E-02$	$1.80E-02$	$1.30E-02$	$\mathbf{0.75E-02}$
		Std	$6.46E+01$	$2.20E+02$	$7.10E+03$	$5.20E+03$	$6.60E-06$	$\mathbf{1.58E-05}$
f_5	0	Mean	$5.60E+02$	$1.60E+03$	$4.60E+02$	$4.12E+02$	$0.02E+00$	$\mathbf{0.01E+00}$
		Std	$1.62E+02$	$2.50E+02$	$2.28E+03$	$0.09E+02$	$1.00E+00$	$\mathbf{0.00E+00}$
f_6	0	Mean	$1.80+01$	$1.59E+01$	$2.30E+01$	$1.00E+01$	$\mathbf{2.78E-06}$	$3.2E-05$
		Std	$3.45E-02$	$3.60E-02$	$6.40E+02$	$2.46E+01$	$\mathbf{0.00E+00}$	$0.01E+01$
f_7	0	Mean	$4.30E+02$	$1.32E+03$	$2.06E+02$	$1.61E+01$	$\mathbf{0.01E+00}$	$\mathbf{0.00E+00}$
		Std	$5.19E+01$	$1.02E+02$	$1.56E+02$	$1.26E+01$	$\mathbf{0.00E+00}$	$\mathbf{0.00E+00}$
f_8	0	Mean	$3.10E+08$	$1.01E+09$	$5.10E+08$	$3.38E+06$	$1.47E+02$	$\mathbf{1.30E+00}$
		Std	$2.10E+08$	$4.54E+08$	$1.90E+08$	$1.09E+07$	$5.30E-06$	$\mathbf{4.70E-05}$

TABLE 4: The survival probability $(1 - Q_{ik})$.

	Ta1	Ta2	Ta3	Ta4	Ta5	Ta6	Ta7	Ta8	Ta9	Ta10
Ua1	0.8923	0.8622	0.8735	0.8147	0.8532	0.8112	0.8209	0.8856	0.8135	0.8326
Ua2	0.8081	0.8576	0.8062	0.8169	0.8682	0.8492	0.8562	0.8775	0.8035	0.8463
Ua3	0.8112	0.8735	0.8862	0.8031	0.8483	0.8855	0.8641	0.8521	0.8940	0.8646
Ua4	0.8132	0.8933	0.8937	0.8625	0.8528	0.8863	0.8422	0.8167	0.8321	0.8031
Ua5	0.8155	0.8618	0.8972	0.8281	0.8437	0.8271	0.8205	0.8389	0.8293	0.8835

TABLE 5: The killing probability (P_{ik}).

	Ta1	Ta2	Ta3	Ta4	Ta5	Ta6	Ta7	Ta8	Ta9	Ta10
Ua1	0.7326	0.7321	0.8815	0.8117	0.7352	0.8972	0.7821	0.7367	0.8791	0.7026
Ua2	0.7718	0.7416	0.7206	0.8705	0.8322	0.8081	0.8935	0.8195	0.7132	0.8793
Ua3	0.8112	0.8810	0.8482	0.8686	0.7661	0.8412	0.8531	0.7603	0.7465	0.8383
Ua4	0.8033	0.8342	0.8462	0.7881	0.8785	0.8988	0.8625	0.7258	0.7110	0.7165
Ua5	0.7662	0.8941	0.8131	0.8106	0.7235	0.7563	0.8211	0.7431	0.7883	0.8613

TABLE 6: The flight range (D_{ik}).

	Ta1	Ta2	Ta3	Ta4	Ta5	Ta6	Ta7	Ta8	Ta9	Ta10
Ua1	20	40	40	30	30	38	28	30	20	40
Ua2	35	35	30	45	29	35	25	20	36	33
Ua3	30	35	26	40	38	45	20	36	32	25
Ua4	25	30	20	20	23	25	36	29	25	30
Ua5	40	25	45	25	35	30	38	25	40	24

TABLE 7: The value of target (E_k).

Ta1	Ta2	Ta3	Ta4	Ta5	Ta6	Ta7	Ta8	Ta9	Ta10
15	60	25	15	80	30	50	65	68	72

TABLE 8: The value of attack aircraft (V_i).

Ua1	Ua2	Ua3	Ua4	Ua5
70	90	80	100	60

FIGURE 2: The comparison of the average performance of each algorithm.

TABLE 9: The performance comparison of the algorithms.

Algorithm	The value of fitness function		The time consumption(s)		
	Optimum	Average	Maximum	Minimum	Average
CRO	297	291	4.6	2.9	3.2
ACA	290	288	3.5	2.2	2.6
SAGA	289	281	3.1	2	2.5
PGA	295	290	2.3	1.4	1.8
PSO	288	284	3.3	2	2.8
CNCRO	302	293	2.2	1.3	1.5

FIGURE 3: The target allocation strategy (the optimal value of fitness function is 302).

the comprehensive analysis results after each algorithm has been run for 25 times are shown in Table 9.

It can be seen from Figure 2 that PGA converges to the best solution after 40 iterations, ACA converges after 81 iterations, CRO converges after 110 iterations, and PSO and SAGA converge after 85 and 83 iterations, respectively, while the CNCRO algorithm in this paper converges to the best solution after 28 iterations. That is to say, CNCRO method has faster convergence speed and better real-time performance.

In Table 9, the fitness value of the objective function of CNCRO is the highest. Based on the maximum overall gain, the minimum loss, and the minimum flight range, compared with other algorithms, CNCRO can obtain greater benefits than other algorithms, and its global optimization ability is stronger which can ensure that the optimal solution is obtained in a short time. Finally, obtain the scheme of target decision-making with the value of fitness function of 302 by using CNCRO, which is shown in Figure 3.

Comprehensively analyze the allocation strategy given in Figure 3. First, by comparing the allocation processes of Ua3 and Ua4 to the target of Ta7 and considering the killing probability of Ta7, Ua4 is slightly better than Ua3, but the difference is small (Ua3 is 0.8531, and Ua4 is 0.8625). Considering the survival probability, Ua3 has a large survival probability (Ua3 is 0.8641, and Ua4 is 0.8422). In addition, in terms of the flight range, Ua3 also has great advantages (20) over Ua4 (36), and the value of attack aircraft of Ua4 (100) is far greater than that of Ua3 (80). Therefore, the algorithm allocates Ta7 to Ua3, to ensure the integrity of high-value aircraft of Ua4, avoid its loss, and keep the path shortest. This allocation scheme is reasonable and effective.

Next, the allocation processes of Ua4 and Ua5 to the target of Ta2 are compared. Compared with other aircraft, Ua4 has the best position to target Ta2; that is, it has a higher survival probability (0.8933), and Ua5 is slightly worse than
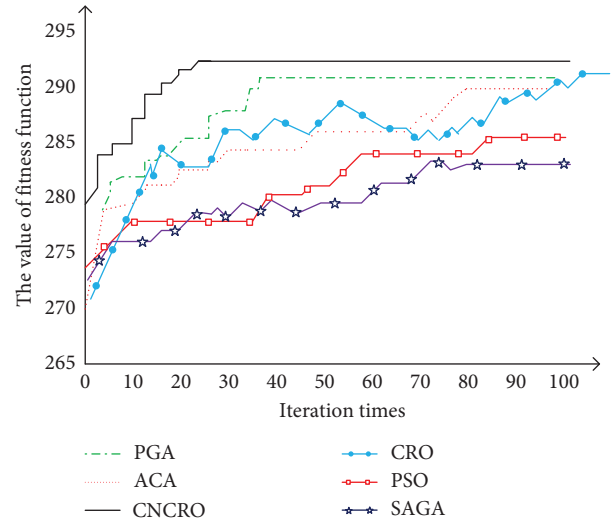
Ua4 (0.8618). However, Ua5 has ammunition advantages; that is, Ua5 has the largest killing probability to Ta2 (0.8941), which is obviously superior to Ua4 (0.8342), and Ta2 has a relatively high value (60). In addition, the flight ranges of Ua4 and Ua5 to the target Ta2 are 30 and 20, respectively. In order to ensure that the aircraft has high survivability, the flight range is as short as possible, and attack the high-value target with the maximum killing probability, Ta2 is allocated to Ua5, to ensure the principle of using superior firepower to

attack the target and avoid the high-risk UAV attacking the high-value target at the same time. That is to say, the attack aircraft with the advantages of position and ammunition will be preferentially allocated to high-value targets to increase the attack income. Meanwhile, the targets with the greater threat should be avoided from being allocated to high-value attack aircraft, which is conducive to the self-preservation of the attack aircraft, and can reduce the loss. On the whole, the CNCRO algorithm can provide a better scheme of cooperative target allocation.

4.2.3. The Influence of Weight Coefficient on UCAV Target Allocation. In the function of UCAV target allocation, three factors will affect the final optimization result, the overall gain, the overall loss, and the total flight range. In order to study the control ability of different factors on the target allocation, the weight coefficients of the overall income, the overall loss, and the total flight range are investigated. The control law of the parameters can guide the determination of the task assignment scheme with different emphases. This part has completed the following three experiments. The parameters of the algorithm are shown in Table 1, and the target allocation parameters of UCAV are shown in Tables 4–8.

(1) To investigate the influence of a single factor, the weight coefficients are set as $\omega_1 = 1, \omega_2 = \omega_3 = 0$ (in consideration of the maximum fitness function). $\omega_1 = 0, \omega_2 = 1, \omega_3 = 0$ (in consideration of the absolute minimum fitness function). $\omega_1 = \omega_2 = 0, \omega_3 = 1$ (in consideration of the absolute minimum fitness function). The experimental results are shown in Tables 10–12.

(2) To investigate the influence of two factors, the weight coefficients are set as $\omega_1 = \omega_2 = 1, \omega_3 = 0$, $\omega_1 = 0, \omega_2 = \omega_3 = 1$, $\omega_1 = 1, \omega_2 = 0, \omega_3 = 1$. The experimental results are shown in Tables 13–15.

(3) The influence of the three factors is investigated. The weight coefficients are set as $\omega_1 = 0.5, \omega_2 = 0.3, \omega_3 = 0.2$. The experimental results are shown in Table 16.

In order to more intuitively investigate the diversity of allocation schemes, the fitness and average error of each experiment are obtained, as shown in Figure 4. The abscissa in the figure represents the target of Ta1–Ta10.

It can be seen from the above charts that when the overall income, the overall loss, and the total flight range are considered separately, the target allocation schemes are quite different, and the performance is relatively divergent with too much diversity. When the two factors are considered at the same time, although the values of fitness function under different combinations are different, the scheme of target allocation has been relatively determined, the aspects considered are more comprehensive, and the algorithm tends to be optimized. When the three factors are considered at the same time, the allocation result is the optimal selection in the previous scheme. Specifically, the allocation schemes of $\omega_1 = 0, \omega_2 = \omega_3 = 1$ and $\omega_1 = 1, \omega_2 = 0, \omega_3 = 1$ in Experiment 2 are the same, and the allocation scheme of $\omega_1 = $

$\omega_2 = 1, \omega_3 = 0$ in Experiment 2 is the same as that of $\omega_1 = 0.5, \omega_2 = 0.3, \omega_3 = 0.2$ in Experiment 3. The main difference between the two schemes is the allocation of Ta3. The former allocates it to Ua4, and the latter allocates it to Ua5. By analyzing the given parameters of Ta3, it can be seen that the killing probability of Ta3 allocated to Ua4 and Ua5 is 0.8462 and 0.8131, respectively, from the perspective of killing probability, assigning Ta3 to Ua4 is more advantageous. In addition, the flight ranges of Ua4 and Ua5 are 20 and 45, respectively. It can be seen that the flight distance of Ua4 is smaller, and the killing efficiency is higher. From the perspective of survival probability, Ua4 and Ua5 are 0.8937 and 0.8972, respectively. Since the parameters of Ua4 and Ua5 are close, the impact on the allocation result can be ignored. In a comprehensive view, the scheme allocated to Ua4 is more optimized.

So, when the optimization conditions are sufficient, although some of the distribution schemes are the same, relatively speaking, the allocation scheme of the three factors will tend to be optimal and more in line with the reality. In addition, the above allocation results are also related to the larger proportion of the total income in the objective function. In the later practical application process, the parameters of the total income, the total loss, the total flight range, and its weight coefficient can be set according to the specific situation, so as to obtain a strategy of target allocation more in line with the actual situation.

4.2.4. The Comparison between Traditional Constrained Processing Technology and Unconstrained Multiobjective Optimization Method. In order to investigate the role of traditional constraint processing technology and unconstrained multiobjective optimization method in the strategy of UCAV target allocation, the two methods are compared experimentally. In addition, since the target allocation scheme of UCAV is closely related to the constraint conditions of C_i (the maximum number of targets that can be attacked by each UAV) and the total number of target set (N) adopted, the experiments in this section mainly use CNCRO algorithm to realize the target allocation based on traditional constrained processing technology and unconstrained multiobjective optimization and control the value of C_i and N, and the performance of the two methods by using C_i and N with different values is investigated. Specifically, it includes two experiments, (1) set C_i as 2, 3, 4, 5, respectively, and the value of the total target number of N is 10, that is, $C_i = 2, 3, 4, 5, N = 10$; (2) the total target set is composed of 5, 6, 7, and 8 targets randomly selected from the original targets, that is, $N = 5, 6, 7, 8, C_i = 3$. In addition, the value of the weight coefficient is $\omega_1 = 0.5, \omega_2 = 0.3, \omega_3 = 0.2$, and the other specific parameter settings are the same as above. The performances of CNCRO in constrained processing and unconstrained multiobjective optimization are obtained by executing 30 times in each case, and the number of times of obtaining the optimal solution in 30 times is shown in Table 17.

It can be seen from Table 17, on the one hand, from the maximum number of targets (C_i), which is a constraint

TABLE 10: The target assignment scheme and fitness function value ($\omega_1 = 1, \omega_2 = \omega_3 = 0$).

UCAV	Ua1	Ua2	Ua3	Ua4	Ua5
Target	Ta3, Ta9	Ta4, Ta7, Ta8, Ta10	Ta1	Ta5, Ta6	Ta2
Optimal fitness	22.0375, 59.7788	13.0575, 44.675, 53.2675, 63.3696	12.168	70.28, 26.964	53.646
Total fitness			419.2439		

TABLE 11: The target assignment scheme and fitness function value ($\omega_1 = 0, \omega_2 = 1, \omega_3 = 0$).

UCAV	Ua1	Ua2	Ua3	Ua4	Ua5
Target	Ta1, Ta8	Ta5	Ta7, Ta9	Ta2, Ta4, Ta6	Ta3, Ta10
Optimal fitness	−7.539, −8.008	−11.862	−10.872, −8.48	−10.67, −13.75, −11.37	−6.168, −6.99
Total fitness			−95.709		

TABLE 12: The target assignment scheme and fitness function value ($\omega_1 = \omega_2 = 0, \omega_3 = 1$).

UCAV	Ua1	Ua2	Ua3	Ua4	Ua5
Target	Ta1, Ta9	Ta8	Ta7	Ta3, Ta4, Ta5, Ta6	Ta2, Ta10
Optimal fitness	−20, −20	−20	−20	−20, −20, −23, −20	−25, −24
Total fitness			−200		

TABLE 13: The target assignment scheme and fitness function value ($\omega_1 = \omega_2 = 1, \omega_3 = 0$).

UCAV	Ua1	Ua2	Ua3	Ua4	Ua5
Target	Ta1, Ta9	Ta8	Ta7	Ta3, Ta4, Ta5, Ta6	Ta2, Ta10
Optimal fitness	2.461, 46.7238	42.2425	31.783	14.1595, −1.9285, 55.56, 15.594	45.354, 55.0236
Total fitness			306.9729		

TABLE 14: The target assignment scheme and fitness function value ($\omega_1 = 0, \omega_2 = \omega_3 = 1$).

UCAV	Ua1	Ua2	Ua3	Ua4	Ua5
Target	Ta1, Ta9	Ta8	Ta7	Ta4, Ta5, Ta6	Ta2, Ta3, Ta10
Optimal fitness	−27.539, −33.055	−31.025	−39.872	−33.75, −34.72, −31.37	−28.292, −30.63, −26.99
Total fitness			317.243		

TABLE 15: The target assignment scheme and fitness function value ($\omega_1 = 1, \omega_2 = 0, \omega_3 = 1$).

UCAV	Ua1	Ua2	Ua3	Ua4	Ua5
Target	Ta1, Ta9	Ta8	Ta7	Ta4, Ta5, Ta6	Ta2, Ta3, Ta10
Optimal fitness	−9.001, 39.7788	33.2675	22.655	−8.1785, 50.28, 6.964	33.646, 1.155, 42.0136
Total fitness			212.5804		

TABLE 16: The target assignment scheme and fitness function value ($\omega_1 = 0.5, \omega_2 = 0.3, \omega_3 = 0.2$).

UCAV	Ua1	Ua2	Ua3	Ua4	Ua5
Target	Ta1, Ta9	Ta8	Ta7	Ta3, Ta4, Ta5, Ta6	Ta2, Ta10
Optimal fitness	1.36, 25.38	21.45	17.63	8.15, −1.285, 27.96, 7.94	26.34, 26.39
Total fitness			306.9729		

condition of the objective function, and it is closely related to the optimization process. The larger the value of C_i, the broader the conditions for controlling the allocation process, the 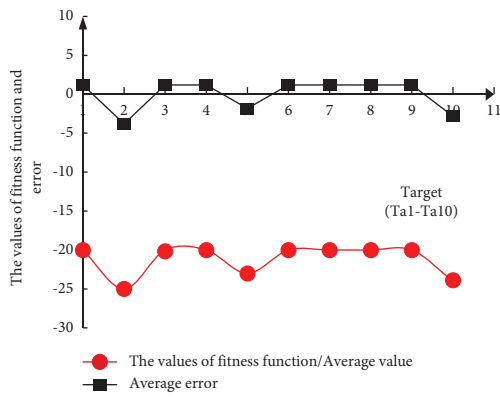simpler the implementation, the greater the possibility of obtaining the optimal solution, and the shorter the execution time. However, when the maximum number of targets is reached, the processing effect and performance will approach saturation or bottleneck. For example, the number of
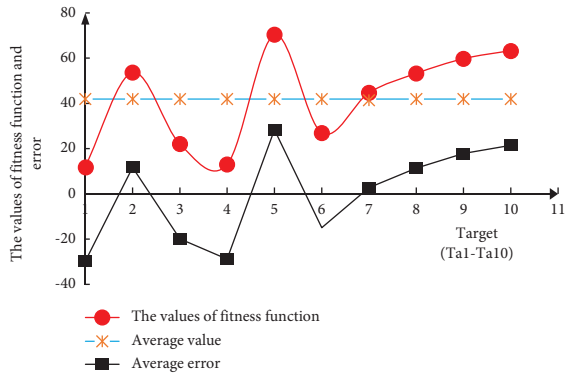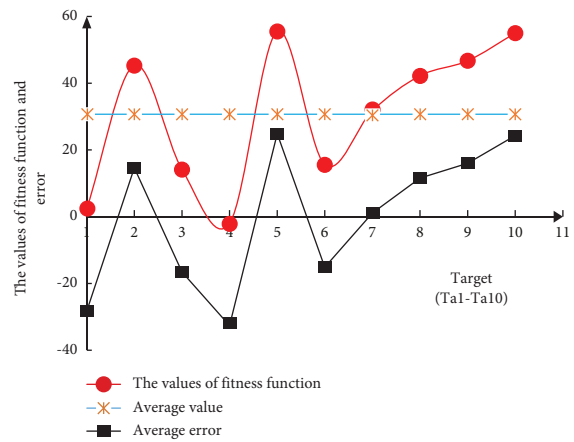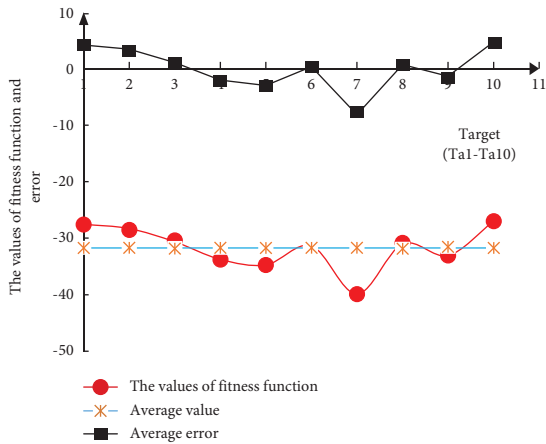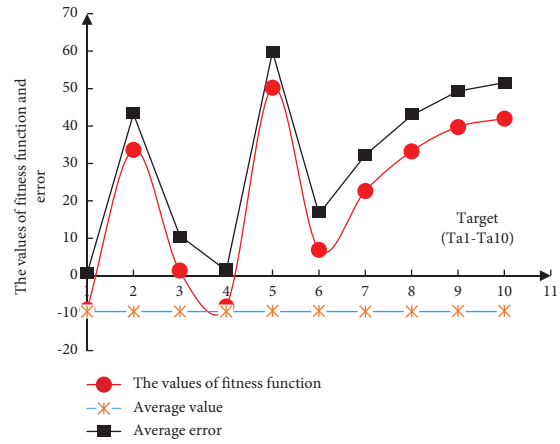
(a)
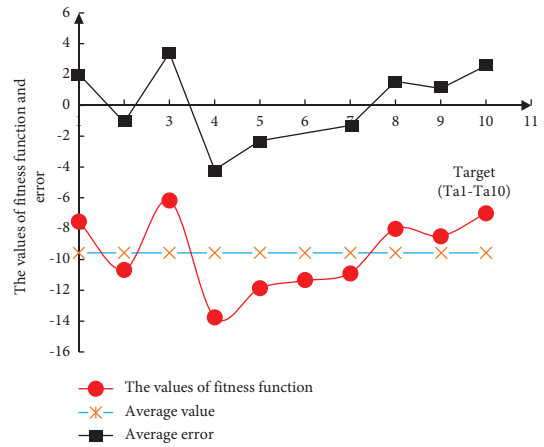
(b)

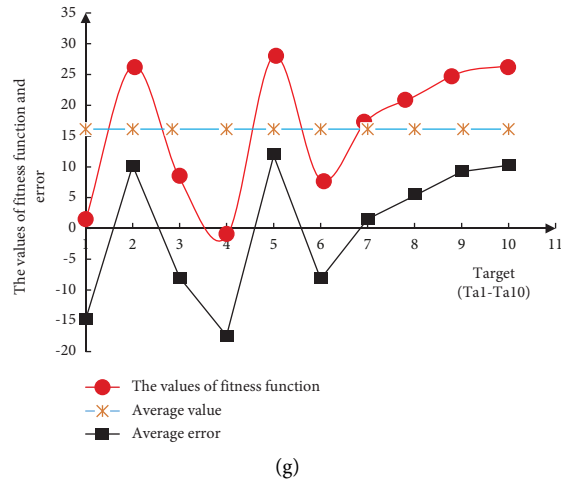

(c)

(d)

(e)

(f)

Figure 4: Continued.

(g)

FIGURE 4: The fitness and average error of each target allocation strategy. (a) The overall income. (b) The overall loss. (c) The total flight range. (d) The overall income and loss. (e) The overall loss and total flight range. (f) The overall income and total flight range. (g) The overall income, loss, and total flight range.

TABLE 17: The performances of CNCRO in constrained processing and unconstrained multiobjective optimization.

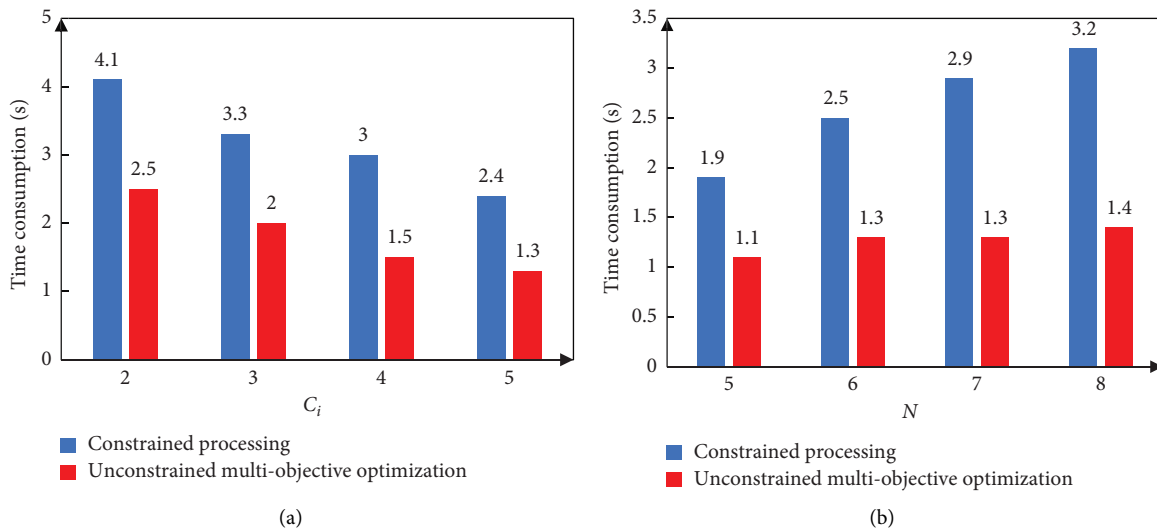| C_i	Constrained processing				Unconstrained multiobjective optimization			
	$C_i = 2$	$C_i = 3$	$C_i = 4$	$C_i = 5$	$C_i = 2$	$C_i = 3$	$C_i = 4$	$C_i = 5$
Optimal times	20	22	26	26	24	26	29	28
N	$N = 5$	$N = 6$	$N = 7$	$N = 8$	$N = 5$	$N = 6$	$N = 7$	$N = 8$
Optimal times	25	23	20	19	28	26	26	25

(a)

(b)
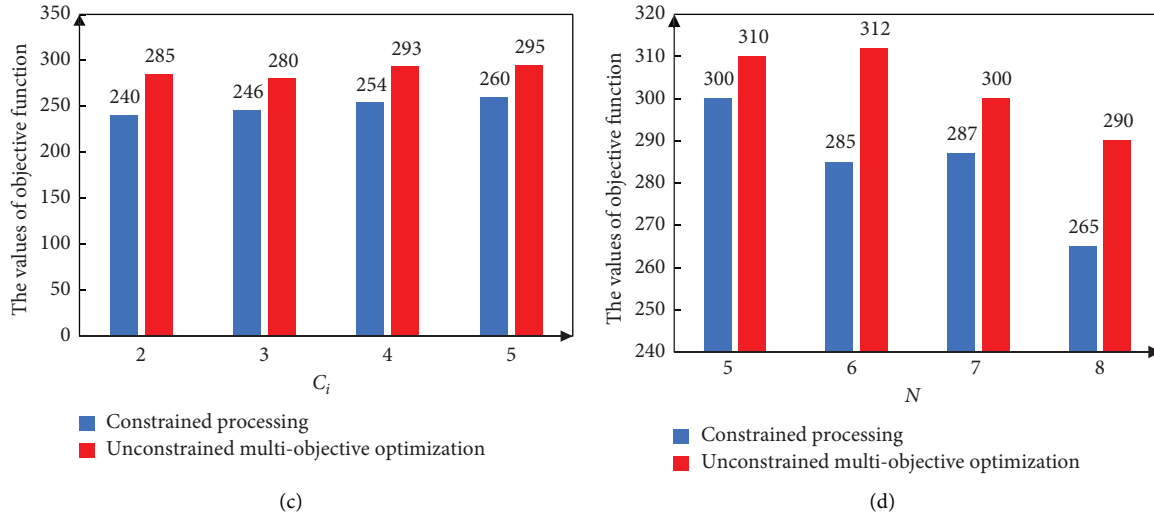
FIGURE 5: Continued.

(c)

(d)

Figure 5: The performance comparison of CNCRO in constrained processing and unconstrained multiobjective optimization. (a) Average time consumption (different C_i). (b) Average time consumption (different N). (c) Average value of objective function (different C_i). (d) Average value of objective function (different N).

times of obtaining optimal solutions is very close for $C_i = 4$ and $C_i = 5$ (26 times for constrained processing and 29 and 28 times for unconstrained multiobjective optimization). On the other hand, from the perspective of the total number of sets (N), the larger value of N will lead to greater difficulty in the implementation process and longer execution time. Therefore, the number of times to obtain optimization will become smaller, which is mainly related to the difficulty of the problem. However, compared with the constrained processing method, the proportion of optimization results obtained by unconstrained multiobjective method will greatly increase.

In addition, the consumption time and the average value of the objective function of the two methods are obtained, as shown in Figure 5.

It can be seen from Figure 5 that the processing time of the unconstrained multiobjective optimization method is shorter than that of the constrained processing method. The main reason is that its optimization process does not need to detect the constraint conditions, and the processing is simpler, more reliable, and with shorter time consumption. In addition, just as the above analysis, the larger the number of maximum targets (C_i), the simpler the implementation process, and the shorter the execution time, while the larger the number of target set (N), the greater the optimization difficulty, and the longer the execution time. As for the value of objective function, on the one hand, the larger the value of C_i, the broader the allocation conditions, the more likely it is to obtain the optimal solution. It also can be seen from Figure 5 that the value of objective function is gradually increased except for isolated cases, which is related to the specific allocation scheme; in addition, when it reaches a certain degree, the processing effect is close to saturation, which is also one of the reasons. However, in general, compared to the constrained processing method, the value of objective function obtained by unconstrained multiobjective optimization

method is better, and its allocation process is more reasonable. On the other hand, the larger the number of set (N), the greater the optimization difficulty. Generally speaking, except for isolated cases, both methods show that the value of objective function gradually decreases with the gradual increase of N, and the optimization difficulty gradually increases.

5. Conclusion

The main innovations of this paper are as follows: (1) by transforming multiple complex constraint conditions into optimization objectives, the constrained optimization problem of UCAV cooperative objective allocation is transformed into a multiobjective optimization problem including allocation objectives and constraint objectives; (2) the energy-reserved chemical reaction algorithm (CNCRO) is proposed. The environmental energy-reserved variable of $buffer$ is introduced into the ineffective collision, combination or splitting reaction between single and multiple molecules of CNCRO to supplement energy for low kinetic energy molecules, to reduce the molecular kinetic energy while ineffective collisions have occurred between molecules. At the same time, the splitting reaction is inspired, to greatly change the molecular structure and promote its search for more solution space, and the global optimization ability is improved; (3) the energy-reserved chemical reaction algorithm (CNCRO) is applied to the process of UCAV cooperative target allocation, the influence of the weight coefficients (ω_1, ω_2, ω_3) of the overall income, the overall loss, and the total flight range in the objective function of UCAV on the allocation scheme is studied, and the influence laws of the maximum number of attack targets (C_i) and the total number of targets (N) on the allocation scheme are obtained, which can lay a foundation for the subsequent implementation of target allocation based on different emphases.

Data Availability

The data used to support the findings of this study are included within the article

Conflicts of Interest

The authors declare no conflicts of interest.

References

[1] F. Wang, H. Zhang, M. C Han, and X. I. N. G. Li-Ning, "Co-Evolution based mixed-variable multi-objective particle swarm optimization for UAV cooperative multi-task allocation problem," *Chinese Journal of Computers*, vol. 44, no. 10, pp. 1967–1983, 2021.

[2] Y. Zhang, D. Lin, D. Zheng, Z. Cheng, and T. A. N. G. Pan, "Task allocation and trajectory optimization of UAV for multi- target time-space synchronization cooperative attack," *Acta Armamentarii*, vol. 42, no. 7, pp. 1482–1495, 2021.

[3] C. H. E. N. Zhi-wang, S. Xia, L. I. Jian-xiong, H. Wang, and W. A. N. G. Chang-meng, "Modeling of unmanned aerial vehicles cooperative target assignment with allocation order and its solving of genetic algorithm," *Control Theory & Applications*, vol. 36, no. 7, pp. 1072–1082, 2019.

[4] C. Zhang and Z. H. A. N. G. Chun, "Research on target assignment modeling and optimization algorithm of anti-aircraft gun anti-UAV," *JOURNAL OF GUN LAUNCH & CONTROL*, vol. 43, no. 02, pp. 15–19, 2022.

[5] Q. Huang, Z. Liu, and J. Tong, "An improved ant colony algorithm for solving firepower allocation problem of USV formation," *Electronics Optics and Control*, vol. 27, no. 8, pp. 58–63, 2020.

[6] S. U. N. Q. Duanxianhua and Caidan, "Optimization assignment for cooperative jamming resources based on improved genetic algorithms," *Journal of Jiangsu University of Science and Technology: Natural Science Edition*, vol. 30, no. 5, pp. 466–472, 2016.

[7] X. Gao, R. Liu, and A. Kaushik, "Hierarchical multi-agent optimization for resource allocation in cloud computing," *IEEE Transactions on Parallel and Distributed Systems*, vol. 32, no. 3, pp. 692–707, 2021.

[8] P. Han and L. Zhang, "Game model and algorithm of Radar jamming resources optimization allocation," *Modern Radar*, vol. 41, no. 2, pp. 78–83, 2019.

[9] C. Yin, R. Yang, W. Zhu et al., "Research on Radio frequency assignment method based on improved genetic algorithm," in *Proceedings of the 2nd International Conference on Artificial Intelligence and Big Data (ICAIBD)*, pp. 358–361, Chengdu, China, September 2019.

[10] J. Yang, "Research on optimized reconfiguration of distributed distribution network based on ant colony optimization algorithm," in *Proceedings of the 2020 International Conference on Computer Engineering and Application (ICCEA)*, pp. 20–23, Guangzhou, China, May 2020.

[11] V. F. Yu, M. Qiu, He Pan, T. P. Chung, and J. N. D. Gupta, "An improved immunoglobulin-based artificial immune system for the aircraft scheduling problem with alternate aircrafts," *IEEE Access*, vol. 9, pp. 16532–16545, 2021.

[12] X. Wang, T. Huang, and Y. Liu, "Resource allocation for random selection of distributed jammer towards multistatic Radar system," *IEEE Access*, vol. 9, pp. 29048–29055, 2021.

[13] H. Xu, B. Song, L. Jiang et al., "An intelligent decision-making algorithm for communication countermeasure jamming resource allocation," *Journal of Electronics and Information Technology*, vol. 43, no. 11, pp. 3086–3095, 2021.

[14] W. Li and G. Qiao, "Compression based distributed dynamic task assignment algorithms for heterogeneous multiple unmanned aerial vehicles," in *Proceedings of the 2017 IEEE International Conference on Robotics and Biomimetics (ROBIO)*, IEEE, Macau, Macao, December 2017.

[15] N. Buckman, H. L. Choi, and J. P. How, "Partial replanning for decentralized dynamic task allocation," in *Proceedings of the AIAA Scitech 2019 Forum*, San Diego, CA, USA, January 2019.

[16] C. Lei, S. T. He, P. Hui et al., "Multiple UAVs hierarchical dynamic task allocation based on PSO-FSA and decentralized auction," in *Proceedings of the 2014 IEEE International Conference on Robotics and Biomimetics (ROBIO 2014)*, IEEE, Bali, Indonesia, December 2014.

[17] H. Yan, W.-D. Bao, Ji Wang, and Da-Yu Zhang, "Multi-UAV cooperative target allocation method based on task relay," *JOURNAL OF COMMAND AND CONTROL*, vol. 7, no. 02, pp. 174–183, 2021.

[18] Y. A. N. G. Fan, T. I. A. N. Wen, and S. O. N. G. Jin, "A multi-objective optimization method of collaborative allocation of route resources," *Computer Simulation*, vol. 38, no. 11, pp. 47–52, 2021.

[19] A. Y. S. Lam and V. O. K. Li, "Chemical-reaction-inspired metaheuristic for optimization," *IEEE Transactions on Evolutionary Computation*, vol. 14, no. 3, pp. 381–399, 2010.

[20] A. Y. S. Lam, V. O. K. Li, and J. J. Q. Yu, "Real-coded chemical reaction optimization," *IEEE Transactions on Evolutionary Computation*, vol. 16, no. 3, pp. 339–353, 2012.

[21] S. Salman and S. Alaswad, "Designing reduced congestion road networks via an elitist adaptive chemical reaction optimization," *Computers & Industrial Engineering*, vol. 163, p. 107788, Article ID 107788, 2022.

[22] R. R. Sahoo and M. Ray, "PSO based test case generation for critical path using improved combined fitness function," *Journal of King Saud University-Computer and Information Sciences*, vol. 32, no. 4, pp. 479–490, 2020.

[23] M. Deng, Z. Wu, Z. Yao, and Y. Chen, "Unmanned aerial vehicle jamming resource scheduling based on parallel genetic algorithm with elite set," *Journal of Electronics and Information Technology*, vol. 44, no. 6, pp. 2158–2165, 2022.

[24] Y. U. Xing-bao, H.-bin Yang, and Yu-feng Zhou, "Design of AGV scheduling system based on simulated annealing genetic algorithm," *Computer Simulation*, vol. 39, no. 5, pp. 76–80+116, 2022.

[25] Y. Wang, M. Chen, L. Xing, Y. Wu, W. Ma, and H. Zhao, "Deep intelligent ant colony optimization for solving travelling salesman problem," *Journal of Computer Research and Development*, vol. 58, no. 8, pp. 1586–1598, 2021.

[26] Y. A. N. G. Song and Q. He, "Real-valued chemical reaction optimization algorithm," *Computer Engineering and Applications*, vol. 52, no. 19, pp. 57–62+145, 2016.